Progress In Electromagnetics Research, PIER 40, 91–111, 2003

ELECTROMAGNETIC SCATTERING BY A MULTILAYER GYROTROPIC BIANISOTROPIC CIRCULAR CYLINDER

M. Zhang, T. S. Yeo, L. W. Li, and M. S. Leong

Antenna and Scattering Laboratory
Department of Electrical and Computer Engineering
National University of Singapore
10 Kent Ridge Crescent, Singapore 119260

Abstract—In this paper, we investigate the electromagnetic scattering by a multilayer gyrotropic bianisotropic circular cylinder in free space. The coupled wave equations of longitudinal field components in the gyrotropic bianisotropic medium are derived. The eigenfunction expansion method is used to solve the scattering problem after uncoupling the coupled wave equations. A 12×12 or 16×16 linear algebraic equation is solved for two cases: one with the center being a perfect electric conducting (PEC) cylinder; and one without the PEC center, respectively. The gyrotropic bianisotropic media can be degenerated into gyrotropic medium, uniaxial bianisotropic medium, biisotropic medium and chiral medium etc. Numerical results presented for the last case was shown to agree exactly with published results. Numerical results of electromagnetic scattering by gyrotropic bianisotropic circular cylinders are presented also.

1 Introduction

2 Formula

2.1 The Wave Equations
2.2 The Eigenfunction Expansion
2.3 Recursive Relationship of Expansion Coefficients

3 Numerical Results

4 Conclusion

References

1. INTRODUCTION

In recent years, increasing interest has been devoted to the basic electromagnetic problems of interaction between electromagnetic waves and complex media [1–15]. The complex media include anisotropic media, chiral media, biisotropic media and bianisotropic media. A gyrotropic bianisotropic medium (GBM) is characterized by the constitutive relations as:

$$\vec{D} = \tilde{\varepsilon} \cdot \vec{E} + \tilde{\xi} \cdot \vec{H}, \tag{1}$$

$$\vec{B} = \tilde{\zeta} \cdot \vec{E} + \tilde{\mu} \cdot \vec{H}, \tag{2}$$

where the constitutive dyadics $\tilde{\varepsilon}, \tilde{\mu}, \tilde{\xi}$, and $\tilde{\zeta}$ all take the form of

$$\tilde{g} = \begin{bmatrix} g_t & -g_c & 0 \\ g_c & g_t & 0 \\ 0 & 0 & g_z \end{bmatrix} \tag{3}$$

In the case of $\tilde{\varepsilon} = \varepsilon\tilde{I}$, $\tilde{\mu} = \mu\tilde{I}$, and $\tilde{\xi} = -\tilde{\zeta} = j\xi_c\tilde{I}$, (3) is reduced to that of a chiral medium. The electromagnetic scattering by a chiral cylinder has been studied in [2, 4–7]. The scattering by a biisotropic cylinder, with $\tilde{\varepsilon} = \varepsilon\tilde{I}$, $\tilde{\mu} = \mu\tilde{I}$, $\tilde{\xi} = \xi\tilde{I}$, and $\tilde{\zeta} = \zeta\tilde{I}$, was studied in [8] using a contour integral technique. If $g_c = 0$, the material is a uniaxial bianisotropic medium. The electromagnetic scattering from a uniaxial bianisotropic cylinder was presented in [9, 10]. Electromagnetic scattering by GBM cylinders of some special shapes has been analysed using equi-volumetric model [11]. In [12], the Beltrami fields were applied to establish the volumetric integral equation for a general bianisotropic medium.

In this paper, we derived the 2-D coupled wave equations of the longitudinal component of electromagnetic fields (E_z, H_z). After a de-coupling process, a pair of Helmholtz equations is obtained. The equations can be solved by the eigenfunction expansion method. By applying the boundary conditions of continuous tangential electric and magnetic fields at the boundary of each layer, the unknown coefficients of expansion eigenfuctions are determined in the recursive form. A 12×12 or 16×16 matrix equation is solved for two cases: one with the center being a perfect electric conducting (PEC) cylinder; and one without the PEC center, respectively. Numerical results, including the bistatic radar cross section and the near-zone fields, are presented for several scatterers.

2. FORMULA

2.1. The Wave Equations

This section presents the derivation of coupled wave equations of E_z and H_z in a GBM and transforming the coupled wave equations to a set of uncoupled wave equations so that eigenfunction expansion can be applied. We assume all fields are time-harmonic with $e^{j\omega t}$ time dependence.

From Maxwell's equations and constitutive relations of a homogeneous GBM which is unbounded and source free, we have

$$\nabla \times \vec{E} = -j\omega(\tilde{\zeta} \cdot \vec{E} + \tilde{\mu} \cdot \vec{H}), \tag{4}$$

$$\nabla \times \vec{H} = j\omega(\tilde{\varepsilon} \cdot \vec{E} + \tilde{\xi} \cdot \vec{H}). \tag{5}$$

All field vectors and the operator ∇ can be decomposited into transverse components denoted by subscript t and longitudinal components denoted by subscript z. Because all fields are uniformed in the longitudinal direction, $\frac{\partial}{\partial z}$ must be zero. After a few simple of vector operations, (4) and (5) can be written as

$$\begin{bmatrix} -\zeta_t & -\mu_t & -\zeta_c & -\mu_c \\ \varepsilon_t & \xi_t & \varepsilon_c & \xi_c \\ \zeta_c & \mu_c & -\zeta_t & -\mu_t \\ -\varepsilon_c & -\xi_c & \varepsilon_t & \xi_t \end{bmatrix} \begin{bmatrix} \vec{E}_t \\ \vec{H}_t \\ \hat{z} \times \vec{E}_t \\ \hat{z} \times \vec{H}_t \end{bmatrix} = \frac{1}{j\omega} \begin{bmatrix} \nabla_t \times E_z \hat{z} \\ \nabla_t \times H_z \hat{z} \\ \nabla_t E_z \\ \nabla_t H_z \end{bmatrix}. \tag{6}$$

Inverting the left-hand side of (6), the relationship between the transverse and longitudinal components of the electromagnetic fields can be written in matrix form as

$$\begin{bmatrix} \vec{E}_t \\ \vec{H}_t \end{bmatrix} = \begin{bmatrix} V_{11} & V_{12} & V_{13} & V_{14} \\ V_{21} & V_{22} & V_{23} & V_{24} \end{bmatrix} \begin{bmatrix} \nabla_t \times E_z \hat{z} \\ \nabla_t \times H_z \hat{z} \\ \nabla_t E_z \\ \nabla_t H_z \end{bmatrix}, \tag{7}$$

where V_{ij} is the element of the inverse matrix of the left-hand side of (6).

Using (4), (5) and (7), the coupled wave equation of E_z and H_z in GBM is

$$\nabla_t^2 \begin{bmatrix} E_z \\ H_z \end{bmatrix} + [T] \begin{bmatrix} E_z \\ H_z \end{bmatrix} = 0, \tag{8}$$

where

$$[T] = [A]^{-1}[B], \tag{9a}$$

$$[A] = \begin{bmatrix} j\omega(\zeta_c V_{13} + \mu_c V_{23}) - 1 & j\omega(\zeta_c V_{14} + \mu_c V_{24}) \\ j\omega(\varepsilon_c V_{13} + \xi_c V_{23}) & j\omega(\varepsilon_c V_{14} + \xi_c V_{24}) + 1 \end{bmatrix}, \tag{9b}$$

$$[B] = \omega^2 \begin{bmatrix} \mu_t\varepsilon_z - \zeta_t\zeta_z & \mu_t\xi_z - \zeta_t\mu_z \\ \xi_t\varepsilon_z - \varepsilon_t\zeta_z & \xi_t\xi_z - \varepsilon_t\mu_z \end{bmatrix}, \tag{9c}$$

Following the works of Bohren [1, 2] and Olyslager [13, 14], the coupling caused by $[T]$ in the coupled wave equation can be removed by diagonalizing $[T]$ such that

$$[a]^{-1}[T][a] = \begin{bmatrix} \gamma_+^2 & 0 \\ 0 & \gamma_-^2 \end{bmatrix} \tag{10}$$

where $[a]$ is the eigenvector matrix of the matrix $[T]$ while γ_+^2 and γ_-^2 are the eigenvalues of the matrix $[T]$. We define (U_+, U_-) by

$$\begin{bmatrix} U_+ \\ U_- \end{bmatrix} = [a]^{-1} \begin{bmatrix} E_z \\ H_z \end{bmatrix}. \tag{11}$$

Substituting (10) and (11) into (8) results in a set of uncoupled equations for U_+ and U_-

$$\nabla_t^2 \begin{bmatrix} U_+ \\ U_- \end{bmatrix} + \begin{bmatrix} \gamma_+^2 & 0 \\ 0 & \gamma_-^2 \end{bmatrix} \begin{bmatrix} U_+ \\ U_- \end{bmatrix} = 0. \tag{12}$$

2.2. The Eigenfunction Expansion

In this section, the eigenfunction expansion for a multilayer GBM cylinder is presented. The geometry of the cylinder is as shown in Fig. 1, where the constitutive dyadics and the outer radius of layer m are $(\tilde{\varepsilon}^{(m)}, \tilde{\mu}^{(m)}, \tilde{\xi}^{(m)}, \tilde{\zeta}^{(m)})$, and ρ_m with $m = 1, 2, \ldots, M$. $\gamma_+^{(m)}$ and $\gamma_-^{(m)}$ denote the eigenvalues of matrix $[T^{(m)}]$ in layer m. The outer radius of the PEC center cylinder, if present, is ρ_0. The external medium is free space, with the constitutive parameters (ε_0, μ_0).

First, consider the fields external to the cylinder. These fields may be expanded as an infinite sum of cylindrical functions, $J_n(\cdot)$ and $H_n^{(2)}(\cdot)$, where $J_n(\cdot)$ is the nth Bessel function of the first kind and $H_n^{(2)}(\cdot)$ is the nth Hankel function of the second kind.

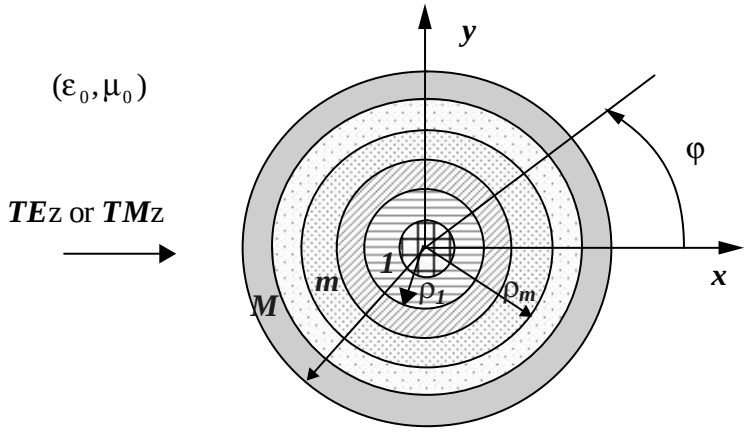

Figure 1. Geometry of a multilayer GBM cylinder with a PEC center.

In the case of a TE or TM polarized plane wave normally incident from $\phi = 180°$, the incident fields may be written as

$$E_z^i = \begin{cases} \sum_{n=0}^{\infty}(2-\delta_{0n})j^{-n}J_n(k_0\rho)\cos(n\phi) & \text{for } TM \\ 0 & \text{for } TE \end{cases}, \tag{13}$$

$$H_z^i = \begin{cases} 0 & \text{for } TM \\ \frac{1}{\eta_0}\sum_{n=0}^{\infty}(2-\delta_{0n})j^{-n}J_n(k_0\rho)\cos(n\phi) & \text{for } TE \end{cases}, \tag{14}$$

$$E_\phi^i = \begin{cases} 0 & \text{for } TM \\ \sum_{n=0}^{\infty}(2-\delta_{0n})j^{-(n-1)}J_n'(k_0\rho)\cos(n\phi) & \text{for } TE \end{cases}, \tag{15}$$

$$H_\phi^i = \begin{cases} \frac{1}{\eta_0}\sum_{n=0}^{\infty}(2-\delta_{0n})j^{-(n+1)}J_n'(k_0\rho)\cos(n\phi) & \text{for } TE \\ 0 & \text{for } TM \end{cases}, \tag{16}$$

where δ_{0n} equals to zero except n is zero, η_0 and k_0 are the wave impedance and wave number in the free space respectively, and the prime indicates the derivative with respect to the argument. Since the constitutive dyadics of the GBM cylinder have non-diagonal elements, the scattering fields will not be symmetrical about $\phi = 0°$. Therefore

the scattered fields will contain both the terms of $\cos(n\phi)$ and $\sin(n\phi)$.

$$E_z^{(M+1)} = \sum_{n=0}^{\infty} H_n^{(2)}(k_0\rho)\left[A_n^{(M+1)}\cos(n\phi) + B_n^{(M+1)}\sin(n\phi)\right], \quad (17)$$

$$H_z^{(M+1)} = \sum_{n=0}^{\infty} H_n^{(2)}(k_0\rho)\left[C_n^{(M+1)}\cos(n\phi) + D_n^{(M+1)}\sin(n\phi)\right], \quad (18)$$

$$E_\phi^{(M+1)} = \sum_{n=0}^{\infty} \frac{-k_0}{j\omega\varepsilon_0} H_n'^{(2)}(k_0\rho)\left[C_n^{(M+1)}\cos(n\phi) + D_n^{(M+1)}\sin(n\phi)\right], \quad (19)$$

$$H_\phi^{(M+1)} = \sum_{n=0}^{\infty} \frac{k_0}{j\omega\mu_0} H_n'^{(2)}(k_0\rho)\left[A_n^{(M+1)}\cos(n\phi) + B_n^{(M+1)}\sin(n\phi)\right]. \quad (20)$$

where the $A_n^{(M+1)}$, $B_n^{(M+1)}$, $C_n^{(M+1)}$, and $D_n^{(M+1)}$ are unknown coefficients.

In layer m of the GMB cylinder, the uncoupled fields $U_+^{(m)}$ and $U_-^{(m)}$ are expanded as infinite sums of $J_n(\cdot)$ and $N_n(\cdot)$, where $N_n(\cdot)$ is the nth Neumann function.

$$\begin{aligned} U_+^{(m)} &= \sum_{n=0}^{\infty} \Big\{ J_n(\gamma_+^{(m)}\rho)\left[A_n^{(m)}\cos(n\phi) + B_n^{(m)}\sin(n\phi)\right] \\ &\quad + N_n(\gamma_+^{(m)}\rho)\left[C_n^{(m)}\cos(n\phi) + D_n^{(m)}\sin(n\phi)\right]\Big\}, \quad (21) \\ U_-^{(m)} &= \sum_{n=0}^{\infty} \Big\{ J_n(\gamma_-^{(m)}\rho)\left[E_n^{(m)}\cos(n\phi) + F_n^{(m)}\sin(n\phi)\right] \\ &\quad + N_n(\gamma_-^{(m)}\rho)\left[G_n^{(m)}\cos(n\phi) + H_n^{(m)}\sin(n\phi)\right]\Big\}, \quad (22) \end{aligned}$$

where the $A_n^{(m)}$, $B_n^{(m)}$, $C_n^{(m)}$, $D_n^{(m)}$, $E_n^{(m)}$, $F_n^{(m)}$, $G_n^{(m)}$ and $H_n^{(m)}$ are unknown coefficients. Using (11) and (7), the longitudinal and transverse tangential components of electromagnetic fields can be written as

$$\begin{aligned} E_z^{(m)} &= a_{11}^{(m)}U_+^{(m)} + a_{12}^{(m)}U_-^{(m)}, \quad (23) \\ H_z^{(m)} &= a_{21}^{(m)}U_+^{(m)} + a_{22}^{(m)}U_-^{(m)}, \quad (24) \end{aligned}$$

$$E_\phi^{(m)} = \sum_{n=1}^{\infty} A_n^{(m)}\left[-S_1^{(m)}\gamma_+^{(m)}J_n'(\gamma_+^{(m)}\rho)\cos(n\phi) - S_2^{(m)}\frac{nJ_n(\gamma_+^{(m)}\rho)}{\rho}\sin(n\phi)\right]$$

$$
\begin{aligned}
&+B_n^{(m)}\left[-S_1^{(m)}\gamma_+^{(m)}J_n'(\gamma_+^{(m)}\rho)\sin(n\phi)+S_2^{(m)}\frac{nJ_n(\gamma_+^{(m)}\rho)}{\rho}\cos(n\phi)\right]\\
&+C_n^{(m)}\left[-S_1^{(m)}\gamma_+^{(m)}N_n'(\gamma_+^{(m)}\rho)\cos(n\phi)-S_2^{(m)}\frac{nN_n(\gamma_+^{(m)}\rho)}{\rho}\sin(n\phi)\right]\\
&+D_n^{(m)}\left[-S_1^{(m)}\gamma_+^{(m)}N_n'(\gamma_+^{(m)}\rho)\sin(n\phi)+S_2^{(m)}\frac{nN_n(\gamma_+^{(m)}\rho)}{\rho}\cos(n\phi)\right]\\
&+E_n^{(m)}\left[-S_3^{(m)}\gamma_-^{(m)}J_n'(\gamma_-^{(m)}\rho)\cos(n\phi)-S_4^{(m)}\frac{nJ_n(\gamma_-^{(m)}\rho)}{\rho}\sin(n\phi)\right]\\
&+F_n^{(m)}\left[-S_3^{(m)}\gamma_-^{(m)}J_n'(\gamma_-^{(m)}\rho)\sin(n\phi)+S_4^{(m)}\frac{nJ_n(\gamma_-^{(m)}\rho)}{\rho}\cos(n\phi)\right]\\
&+G_n^{(m)}\left[-S_3^{(m)}\gamma_-^{(m)}N_n'(\gamma_-^{(m)}\rho)\cos(n\phi)-S_4^{(m)}\frac{nN_n(\gamma_-^{(m)}\rho)}{\rho}\sin(n\phi)\right]\\
&+H_n^{(m)}\left[-S_3^{(m)}\gamma_-^{(m)}N_n'(\gamma_-^{(m)}\rho)\sin(n\phi)+S_4^{(m)}\frac{nN_n(\gamma_-^{(m)}\rho)}{\rho}\cos(n\phi)\right],
\end{aligned}
\tag{25}
$$

$$
\begin{aligned}
&H_\phi^{(m)}=\\
&\sum_{n=1}^{\infty}A_n^{(m)}\left[-S_5^{(m)}\gamma_+^{(m)}J_n'(\gamma_+^{(m)}\rho)\cos(n\phi)-S_6^{(m)}\frac{nJ_n(\gamma_+^{(m)}\rho)}{\rho}\sin(n\phi)\right]\\
&+B_n^{(m)}\left[-S_5^{(m)}\gamma_+^{(m)}J_n'(\gamma_+^{(m)}\rho)\sin(n\phi)+S_6^{(m)}\frac{nJ_n(\gamma_+^{(m)}\rho)}{\rho}\cos(n\phi)\right]\\
&+C_n^{(m)}\left[-S_5^{(m)}\gamma_+^{(m)}N_n'(\gamma_+^{(m)}\rho)\cos(n\phi)-S_6^{(m)}\frac{nN_n(\gamma_+^{(m)}\rho)}{\rho}\sin(n\phi)\right]\\
&+D_n^{(m)}\left[-S_5^{(m)}\gamma_+^{(m)}N_n'(\gamma_+^{(m)}\rho)\sin(n\phi)+S_6^{(m)}\frac{nN_n(\gamma_+^{(m)}\rho)}{\rho}\cos(n\phi)\right]\\
&+E_n^{(m)}\left[-S_7^{(m)}\gamma_-^{(m)}J_n'(\gamma_-^{(m)}\rho)\cos(n\phi)-S_8^{(m)}\frac{nJ_n(\gamma_-^{(m)}\rho)}{\rho}\sin(n\phi)\right]
\end{aligned}
$$

$$+F_n^{(m)}\left[-S_7^{(m)}\gamma_-^{(m)}J_n'(\gamma_-^{(m)}\rho)\sin(n\phi)+S_8^{(m)}\frac{nJ_n(\gamma_-^{(m)}\rho)}{\rho}\cos(n\phi)\right]$$
$$+G_n^{(m)}\left[-S_7^{(m)}\gamma_-^{(m)}N_n'(\gamma_-^{(m)}\rho)\cos(n\phi)-S_8^{(m)}\frac{nN_n(\gamma_-^{(m)}\rho)}{\rho}\sin(n\phi)\right]$$
$$+H_n^{(m)}\left[-S_7^{(m)}\gamma_-^{(m)}N_n'(\gamma_-^{(m)}\rho)\sin(n\phi)+S_8^{(m)}\frac{nN_n(\gamma_-^{(m)}\rho)}{\rho}\cos(n\phi)\right], \tag{26}$$

where $a_{ij}^{(m)}$ is the element of matrix defined in (10), and $S_i^{(m)}, i = 1, 2, \ldots, 8$ are defined as

$$\begin{bmatrix} S_1^{(m)} & S_3^{(m)} \\ S_5^{(m)} & S_7^{(m)} \end{bmatrix} = \begin{bmatrix} V_{11}^{(m)} & V_{12}^{(m)} \\ V_{21}^{(m)} & V_{22}^{(m)} \end{bmatrix} \begin{bmatrix} a_{11}^{(m)} & a_{12}^{(m)} \\ a_{21}^{(m)} & a_{22}^{(m)} \end{bmatrix}$$
$$\text{and} \begin{bmatrix} S_2^{(m)} & S_4^{(m)} \\ S_6^{(m)} & S_8^{(m)} \end{bmatrix} = \begin{bmatrix} V_{13}^{(m)} & V_{14}^{(m)} \\ V_{23}^{(m)} & V_{24}^{(m)} \end{bmatrix} \begin{bmatrix} a_{11}^{(m)} & a_{12}^{(m)} \\ a_{21}^{(m)} & a_{22}^{(m)} \end{bmatrix}.$$

Note that the fields in each layer of the GBM cylinder are expanded in terms of 8 unknowns, $A_n^{(m)}$ to $H_n^{(m)}$. It differs from a chiral medium [5], where only 4 unknowns are required. This is because the fields in GBM cylinder are asymmetrical about $\phi = 0°$, although the problem is geometric symmetry.

If the center cylinder is a GBM cylinder, the uncoupled fields $U_+^{(0)}$ and $U_-^{(0)}$ are expanded as infinite sums of $J_n(\cdot)$. Therefore the expansion coefficients $C_n^{(0)}$, $D_n^{(0)}$, $G_n^{(0)}$, and $H_n^{(0)}$, in (21) and (22) must be zero.

2.3. Recursive Relationship of Expansion Coefficients

This section presents the recursive technique for determining the coefficients of the eigenfunction expansions. These unknowns include $A_n^{(m)}$, $B_n^{(m)}$, $C_n^{(m)}$, $D_n^{(m)}$, $E_n^{(m)}$, $F_n^{(m)}$, $G_n^{(m)}$ and $H_n^{(m)}$ in each of the M layers, $A_n^{(M+1)}$, $B_n^{(M+1)}$, $C_n^{(M+1)}$, and $D_n^{(M+1)}$ in free space as well as $A_n^{(0)}$, $B_n^{(0)}$, $E_n^{(0)}$, and $F_n^{(0)}$ in the case of the center cylinder is also a GBM cylinder. The unknown coefficients are determined by applying the boundary conditions of continuous tangential electric and magnetic fields at the boundary of each layer. The resulting relationship between

the coefficients for layers m and $m+1$ can be represented in matrix form by

$$\begin{bmatrix} A_n^{(m+1)} \\ \vdots \\ H_n^{(m+1)} \end{bmatrix} = \left[y_1^{(m+1)}\right]^{-1} \left[y_0^{(m)}\right] \begin{bmatrix} A_n^{(m)} \\ \vdots \\ H_n^{(m)} \end{bmatrix} = \left[Y^{(m)}\right] \begin{bmatrix} A_n^{(m+1)} \\ \vdots \\ H_n^{(m+1)} \end{bmatrix}, \quad (27)$$

where $[y_0^{(m)}]$ is an 8×8 matrix, which is

$$\begin{bmatrix}
a_{11}^{(m)} J_n^+ & 0 & a_{11}^{(m)} N_n^+ & 0 \\
0 & a_{11}^{(m)} J_n^+ & 0 & a_{11}^{(m)} N_n^+ \\
-S_1^{(m)} \gamma_+^{(m)} J_n'^+ & S_2^{(m)} n J_n^+ / \rho_m & -S_1^{(m)} \gamma_+^{(m)} N_n'^+ & S_2^{(m)} n N_n^+ / \rho_m \\
-S_2^{(m)} n J_n^+ / \rho_m & -S_1^{(m)} \gamma_+^{(m)} J_n'^+ & -S_2^{(m)} n N_n^+ / \rho_m & -S_1^{(m)} \gamma_+^{(m)} N_n'^+ \\
a_{21}^{(m)} J_n^+ & 0 & a_{21}^{(m)} N_n^+ & 0 \\
0 & a_{21}^{(m)} J_n^+ & 0 & a_{21}^{(m)} N_n^+ \\
-S_5^{(m)} \gamma_+^{(m)} J_n'^+ & S_6^{(m)} n J_n^+ / \rho_m & -S_5^{(m)} \gamma_+^{(m)} N_n'^+ & S_6^{(m)} n N_n^+ / \rho_m \\
-S_6^{(m)} n J_n^+ / \rho_m & -S_5^{(m)} \gamma_+^{(m)} J_n'^+ & -S_6^{(m)} n N_n^+ / \rho_m & -S_5^{(m)} \gamma_+^{(m)} N_n'^+
\end{bmatrix}$$

$$\begin{bmatrix}
a_{12}^{(m)} J_n^- & 0 & a_{12}^{(m)} N_n^- & 0 \\
0 & a_{12}^{(m)} J_n^- & 0 & a_{12}^{(m)} N_n^- \\
-S_3^{(m)} \gamma_-^{(m)} J_n'^- & S_4^{(m)} n J_n^- / \rho_m & -S_3^{(m)} \gamma_-^{(m)} N_n'^- & S_4^{(m)} n N_n^- / \rho_m \\
-S_4^{(m)} n J_n^- / \rho_m & -S_3^{(m)} \gamma_+^{(m)} J_n'^+ & -S_4^{(m)} n N_n^- / \rho_m & -S_3^{(m)} \gamma_+^{(m)} N_n'^+ \\
a_{22}^{(m)} J_n^- & 0 & a_{22}^{(m)} N_n^- & 0 \\
0 & a_{22}^{(m)} J_n^- & 0 & a_{22}^{(m)} N_n^- \\
-S_7^{(m)} \gamma_-^{(m)} J_n'^- & S_8^{(m)} n J_n^- / \rho_m & -S_7^{(m)} \gamma_-^{(m)} N_n'^- & S_8^{(m)} n N_n^- / \rho_m \\
-S_8^{(m)} n J_n^- / \rho_m & -S_7^{(m)} \gamma_+^{(m)} J_n'^+ & -S_8^{(m)} n N_n^- / \rho_m & -S_7^{(m)} \gamma_+^{(m)} N_n'^+
\end{bmatrix}$$

with J_n^+, J_n^-, $J_n'^+$, and $J_n'^-$ denote Bessel function $J_n(\gamma_+^{(m)}\rho_m)$, $J_n(\gamma_-^{(m)}\rho_m)$, $\frac{\partial J_n(\gamma_+^{(m)}\rho_m)}{\partial(\gamma_+^{(m)}\rho_m)}$, and $\frac{\partial J_n(\gamma_-^{(m)}\rho_m)}{\partial(\gamma_-^{(m)}\rho_m)}$ respectively, and so do Neumann functions, $[y_1^{(m+1)}] = [y_0^{(m+1)}(\rho_{m+1} \to \rho_m)]$.

The recursive relationship between the unknown coefficients for

layer m and layer 1 can be written as

$$\begin{bmatrix} A_n^{(M)} \\ \vdots \\ H_n^{(M)} \end{bmatrix} = \left[Y^{(M-1)}\right]\left[Y^{(M-2)}\right]\cdots\left[Y^{(1)}\right]\begin{bmatrix} A_n^{(1)} \\ \vdots \\ H_n^{(1)} \end{bmatrix} = [X]\begin{bmatrix} A_n^{(1)} \\ \vdots \\ H_n^{(1)} \end{bmatrix}, \tag{28}$$

where $[Y^{(m)}]$, $m = 1, 2, \ldots, M-1$, are defined in (27).

Applying the boundary conditions between the M layer and exterior free space, a linear algebraic equation can be obtained

$$\begin{bmatrix}\left[y_0^{(M)}\right] - \left[x_1^{(M+1)}\right]\end{bmatrix}\begin{bmatrix} A_n^{(M)} & \ldots & H_n^{(M)} & A_n^{(M+1)} & \ldots & D_N^{(M+1)} \end{bmatrix}^T = \left[[b][0]\right]^T, \tag{29}$$

where $[0]$ is a 4-element vector, and $[b]$ is a 8-element vector

$$[b] = \begin{cases} \begin{bmatrix} (2-\delta_{0n})j^{-n}J_n(k_0\rho_M) & 0 & 0 & 0 \\ 0 & 0 & (2-\delta_{0n})j^{-(n-1)}J_n'(k_0\rho_M) & 0 \end{bmatrix}^T & \text{for } TM \\ \begin{bmatrix} 0 & 0 & (2-\delta_{0n})j^{-(n-1)}J_n'(k_0\rho_M)/\eta_0 & 0 \\ & & (2-\delta_{0n})j^{-n}J_n(k_0\rho_M)/\eta_0 & 0 & 0 & 0 \end{bmatrix}^T & \text{for } TE \end{cases},$$

and $[x_1^{(M+1)}]$ is a 8×4 matrix,

$$\begin{bmatrix} H_n^{(2)}(k_0\rho_M) & 0 & 0 & 0 \\ 0 & H_n^{(2)}(k_0\rho_M) & 0 & 0 \\ 0 & 0 & j\eta_0 H_n'^{(2)}(k_0\rho_M) & 0 \\ 0 & 0 & 0 & j\eta_0 H_n'^{(2)}(k_0\rho_M) \\ 0 & 0 & H_n^{(2)}(k_0\rho_M) & 0 \\ 0 & 0 & 0 & H_n^{(2)}(k_0\rho_M) \\ \frac{1}{j\eta_0}H_n'^{(2)}(k_0\rho_M) & 0 & 0 & 0 \\ 0 & \frac{1}{j\eta_0}H_n'^{(2)}(k_0\rho_M) & 0 & 0 \end{bmatrix}.$$

When the center cylinder is a GBM cylinder, applying boundary conditions on the interface between layer 1 and center cylinder, we

obtain

$$\begin{bmatrix} A_n^{(1)} \\ \vdots \\ H_n^{(1)} \end{bmatrix} = \left[y_1^{(1)}\right]^{-1} \left[x_0^{(0)}\right] \begin{bmatrix} A_n^{(0)} \\ B_n^{(0)} \\ E_n^{(0)} \\ F_n^{(0)} \end{bmatrix}, \tag{30}$$

where $[x_0^{(0)}]$ is a 8×4 matrix, defined by $[y_0^{(0)}]$ as $[x_0^{(0)}]_{ij} = [y_0^{(0)}]_{il}$ for $i = 1, 2, \ldots, 8$; $j = 1, 2, 3, 4 \Rightarrow l = 1, 2, 5, 6$. From (28), (29) and (30), a 16×16 matrix equation is obtained

$$\begin{aligned} &\begin{bmatrix} [y_0^{(M)}]_{8\times 8} & -[x_1^{(M+1)}]_{8\times 4} & [0]_{8\times 4} \\ [y_1^{(1)}]_{8\times 8}[X]_{8\times 8}^{-1} & [0]_{8\times 4} & -[x_0^{(0)}]_{8\times 4} \end{bmatrix}. \\ &\begin{bmatrix} A_n^{(M)} \ldots H_n^{(M)} & A_n^{(M+1)} \ldots D_n^{(M+1)} & A_n^{(0)} & B_n^{(0)} & E_n^{(0)} & F_n^{(0)} \end{bmatrix}_{16\times 1}^T \\ = \quad & [[b]_{8\times 1} \quad [0]_{8\times 1}]^T. \end{aligned} \tag{31}$$

When the center cylinder is a PEC cylinder, boundary conditions require that the tangential electric fields to be zero, we obtain

$$\left[x_1^{(1)}\right] \begin{bmatrix} A_n^{(1)} \\ \vdots \\ H_n^{(1)} \end{bmatrix} = 0, \tag{32}$$

where $[x_1^{(1)}]$ is a 4×8 matrix, defined by $[y_1^{(1)}]$ as $[x_1^{(1)}]_{ij} = [y_1^{(1)}]_{ij}$ for $i = 1, 2, 3, 4$; $j = 1, 2, \ldots, 8$.

From (28), (29) and (32), a 12×12 matrix equation is obtained

$$\begin{aligned} &\begin{bmatrix} [y_0^{(M)}]_{8\times 8} & -[x_1^{(M+1)}]_{8\times 4} \\ [x_1^{(1)}]_{4\times 8}[X]_{8\times 8}^{-1} & [0]_{8\times 4} \end{bmatrix}. \\ &\begin{bmatrix} A_n^{(M)} & \ldots & H_n^{(M)} & A_n^{(M+1)} & \ldots & D_n^{(M+1)} \end{bmatrix}_{12\times 1}^T \\ = \quad & [[b]_{8\times 1} \quad [0]_{8\times 1}]^T. \end{aligned} \tag{33}$$

(31) and (33) define the unknown coefficients required to calculate the scattered fields and internal fields.

For the 2-D scattering problem, the radar cross section (RCS) is defined as

$$\sigma = \lim_{\rho\to\infty} 2\pi\rho \frac{|E^s|^2}{|E^i|^2}. \tag{34}$$

In scattering by a GBM cylinder, cross-polarized scattered field will be excited due to the non-isotropic nature of its constitutive parameters. The co-polarized and cross-polarized RCS can be defined and evaluated as

$$\begin{aligned}
\sigma_{co} &= \lim_{\rho\to\infty} 2\pi\rho \frac{|E_z^s|^2}{|E_z^i|^2} \\
&= \frac{4}{k_0}\left|\sum_{n=0}^{\infty} j^n \left[A_n^{(M+1)}\cos(n\phi) + B_n^{(M+1)}\sin(n\phi)\right]\right|^2 \\
\sigma_{cross} &= \lim_{\rho\to\infty} 2\pi\rho \frac{|E_\phi^s|^2}{|E_z^i|^2} \\
&= \frac{4\eta_0^2}{k_0}\left|\sum_{n=0}^{\infty} j^{n-1} \left[C_n^{(M+1)}\cos(n\phi) + D_n^{(M+1)}\sin(n\phi)\right]\right|^2 \\
&\qquad\qquad \text{for } TM, \qquad (35)
\end{aligned}$$

and

$$\begin{aligned}
\sigma_{co} &= \lim_{\rho\to\infty} 2\pi\rho \frac{|H_z^s|^2}{|H_z^i|^2} \\
&= \frac{4\eta_0^2}{k_0}\left|\sum_{n=0}^{\infty} j^n \left[C_n^{(M+1)}\cos(n\phi) + D_n^{(M+1)}\sin(n\phi)\right]\right|^2 \\
\sigma_{cross} &= \lim_{\rho\to\infty} 2\pi\rho \frac{|H_\phi^s|^2}{|H_z^i|^2} \\
&= \frac{4}{k_0}\left|\sum_{n=0}^{\infty} j^{n-1} \left[A_n^{(M+1)}\cos(n\phi) + B_n^{(M+1)}\sin(n\phi)\right]\right|^2 \\
&\qquad\qquad \text{for } TE. \qquad (36)
\end{aligned}$$

3. NUMERICAL RESULTS

This section presents the numerical results for TM and TE scattering by five different cylinders in free space. The results include bistatic RCS and near-zone electric and magnetic fields. The frequency of the incident wave is taken to be 300 MHz in all cases.

First, the TM ($\vec{E}^i = \hat{z}e^{-jk_0x}$) scattering by a two-layer chiral cylinder with and without a PEC center cylinder was analysed and compared with results obtained from [5]. As the constitutive

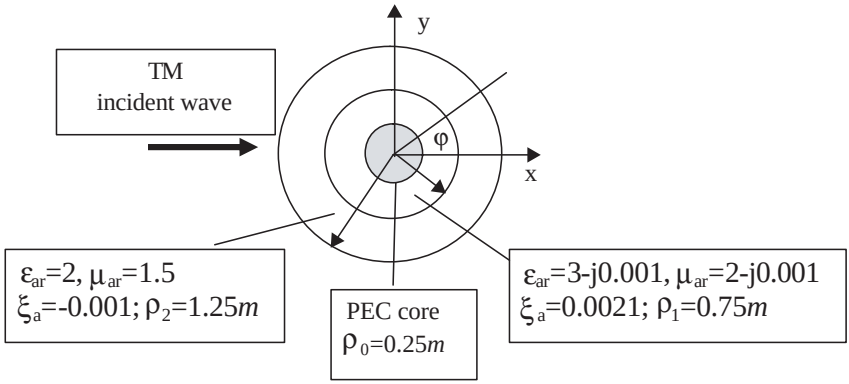

Figure 2. A two-layer chiral cylinder with a PEC center.

parameters have been defined differently, the following conversion relation was applied: $\tilde{\varepsilon} = (\varepsilon_a + \mu_a \xi_a^2)\tilde{I}$, $\tilde{\mu} = \mu_a \tilde{I}$, $\tilde{\xi} = j\mu_a \xi_a \tilde{I}$ and $\tilde{\zeta} = -j\mu_a \xi_a \tilde{I}$, where $\tilde{\varepsilon}$, $\tilde{\mu}$, $\tilde{\xi}$, and $\tilde{\zeta}$ are the parameters taken in this paper, ε_a, μ_a and ξ_a are the parameters used in [5].

Fig. 3(a) shows the co-polarized and cross-polarized bistatic RCS of the chiral cylinder. Fig. 3(b) shows the bistatic RCS of this cylinder with the PEC center cylinder replaced by the same material as the inner layer chiral cylinder. The RCS curves are identical as those in [5] as it can be shown easily that our formulation collapses to that of [5] in the case of chiral medium.

The second example is the scattering of TM and TE polarized incident plane waves by a circular GBM cylinder. The radius of the cylinder is taken to be 1 m, The cylinder is lossy in nature and its parameters are: $\varepsilon_t = (2-j0.5)\varepsilon_0$, $\varepsilon_z = (3-j1.5)\varepsilon_0$, $\varepsilon_c = (0.5-j0.2)\varepsilon_0$, $\mu_t = (4 - j0.05)\mu_0$, $\mu_z = (2 - j0.1)\mu_0$, $\mu_c = (0.3 - j0.1)\mu_0$, $\xi_t = (1 - j0.1)\sqrt{\varepsilon_0\mu_0}$, $\xi_z = (0.8 - j0.2)\sqrt{\varepsilon_0\mu_0}$, $\xi_c = (0.5 - j0.1)\sqrt{\varepsilon_0\mu_0}$, $\zeta_t = (-0.1 - j0.9)\sqrt{\varepsilon_0\mu_0}$, $\zeta_z = (-0.2 - j0.8)\sqrt{\varepsilon_0\mu_0}$, $\zeta_c = (0.3 - j0.2)\sqrt{\varepsilon_0\mu_0}$. Fig. 4(a) shows the co-polarized and cross-polarized bistatic RCS of this cylinder for a TM incident plane wave. The near-zone electric and magnetic fields along x-axis are shown in Figs. 4(b) and 4(c) respectively. Fig. 5 shows the co-polarized and cross-polarized bistatic RCS and near-zone electric and magnetic fields along x-axis of this cylinder for a TE incident plane wave.

It is seen from these results that, unlike the case for scattering by a unaxial bianisotropic circular cylinder in [9] and next example, the co- and cross-polarization radar cross section of a GEM circular cylinder is not symmetrical with respect to the scattering angle ϕ, due to the existence of nonzero non-diagonal, elements in the constitutive

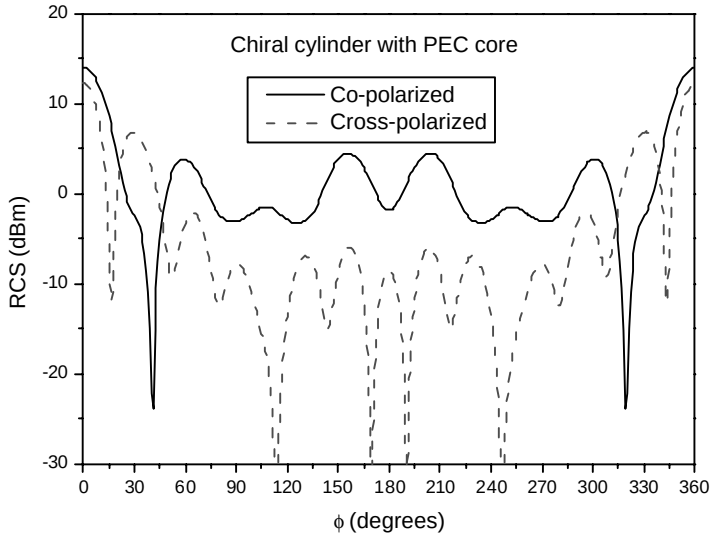

(a)

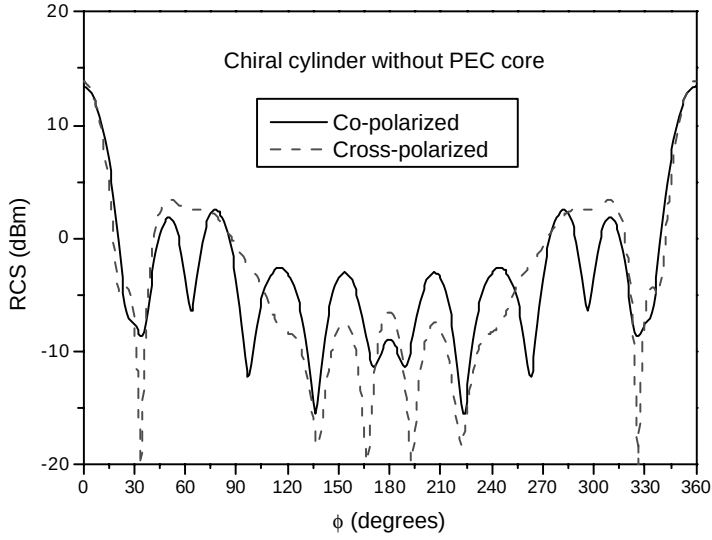

(b)

Figure 3. The co-polarized and cross-polarized bistatic RCS of a two-layer chiral cylinder (a) with and (b) without PEC center cylinder for a TM incident plane wave.

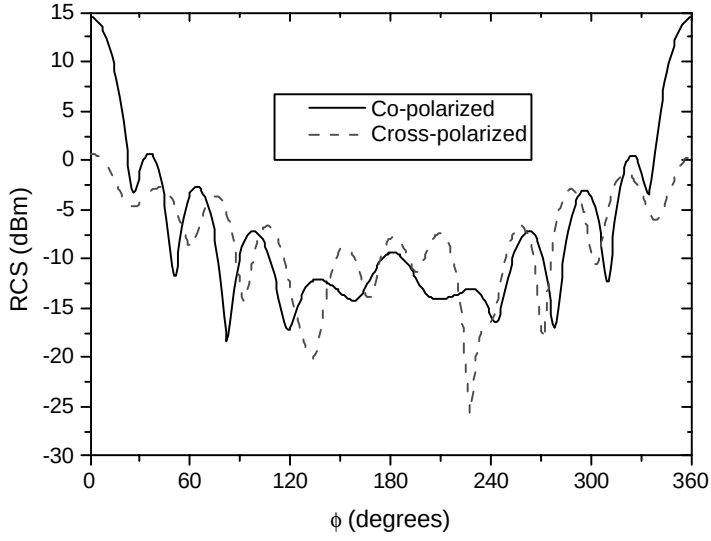
Co-polarized
Cross-polarized
RCS (dBm)
ϕ (degrees)
15
10
5
0
-5
-10
-15
-20
-25
-30
0
60
120
180
240
300
360

(a)

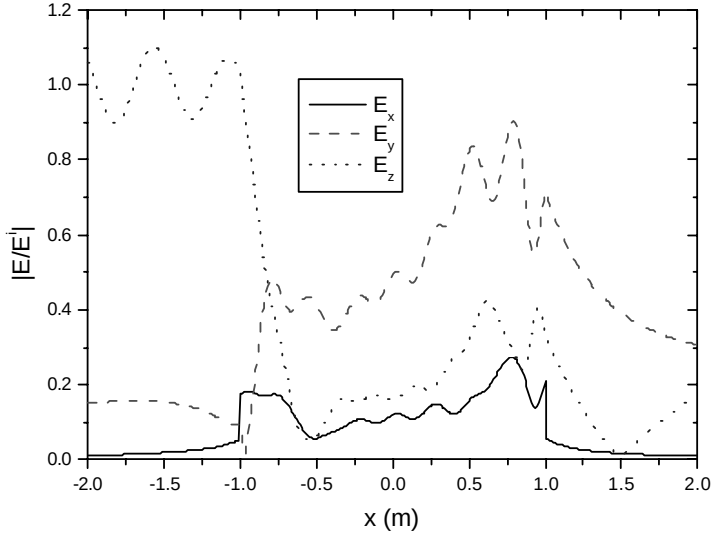
E_x
E_y
E_z
|E/E^i|
x (m)
1.2
1.0
0.8
0.6
0.4
0.2
0.0
-2.0
-1.5
-1.0
-0.5
0.0
0.5
1.0
1.5
2.0

(b)

Figure 4.

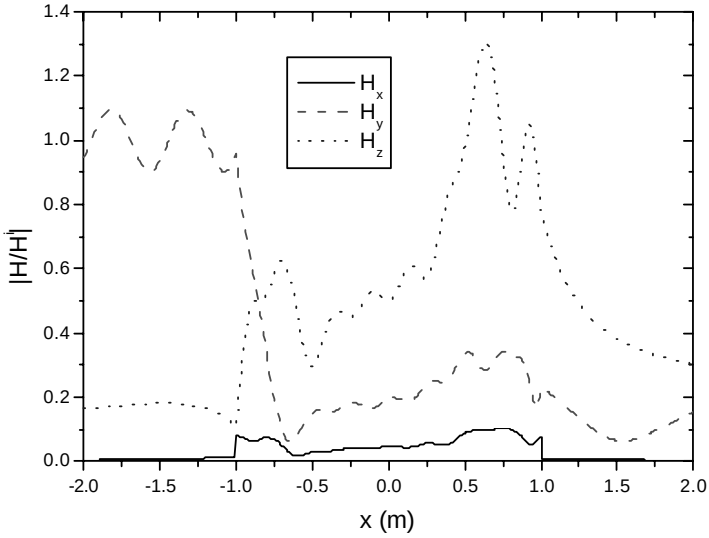

(c)

Figure 4. The co-polarized and cross-polarized bistatic RCS (a) and near-zone electric (b) and magnetic (c) fields of a GBM cylinder for a TM incident plane wave.

relation, although the problem is geometric symmetry. Also, the cross-polarized radar cross sections for the TM and TE cases are not identical, unlike the chiral medium case [5], due to the irreciprocal property of the constitutive parameters. Along the $-x$ direction, the E_z and H_y components for TM case and H_z and E_y components for TE case, dominate the electric and magnetic fields, respectively. The co-polarized components penetrate into, and peaked within, the cylinder. However, once outside, they decay rapidly. On the other hand, the cross-polarized components, E_y and H_z components for TM-case and H_y and E_z components for TE-case, decay only at a much slower rate. In all cases, the E_x and H_x components do not contribute significantly to the total electromagnetic fields both inside and outside of the cylinder. It is also observed that after the incident wave enters into the cylinder, the contribution of all the components due to the incident wave is increased, especially at around the second interface.

The third example presented here is the TE scattering of a two-layer uniaxial bianisotropic cylinder with and without a PEC center cylinder. The cylinder (Fig. 6) has an outer radius of 1 meter (one wavelength). Fig. 7(a) shows the co-polarized and cross-polarized bistatic RCS of this cylinder for a TE incident plane wave. Fig. 7(b)

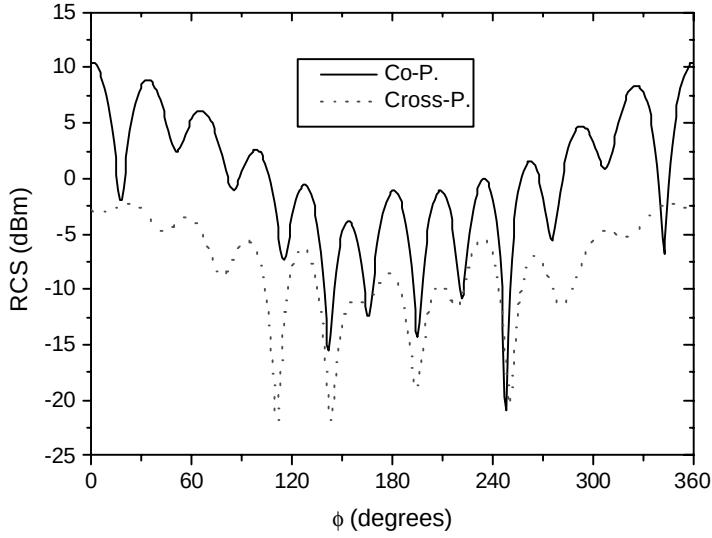
Co-P.
Cross-P.
RCS (dBm)
ϕ (degrees)
15
10
5
0
-5
-10
-15
-20
-25
0
60
120
180
240
300
360

(a)

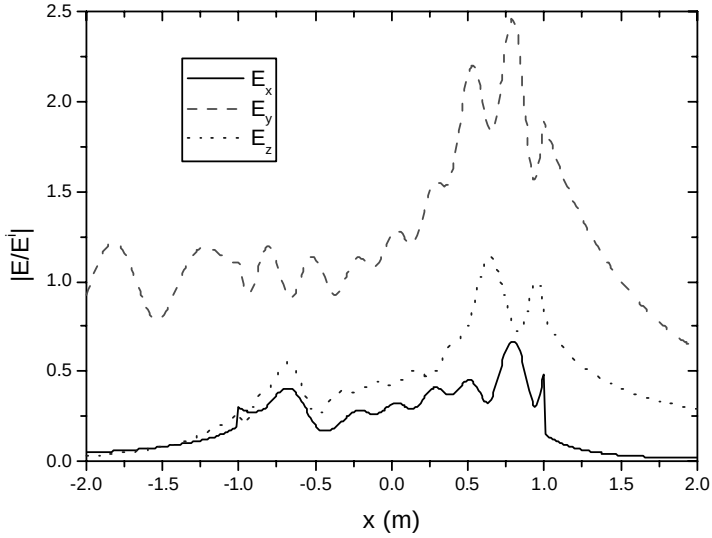
E_x
E_y
E_z
|E/E^i|
x (m)
2.5
2.0
1.5
1.0
0.5
0.0
-2.0
-1.5
-1.0
-0.5
0.0
0.5
1.0
1.5
2.0

(b)

Figure 5.

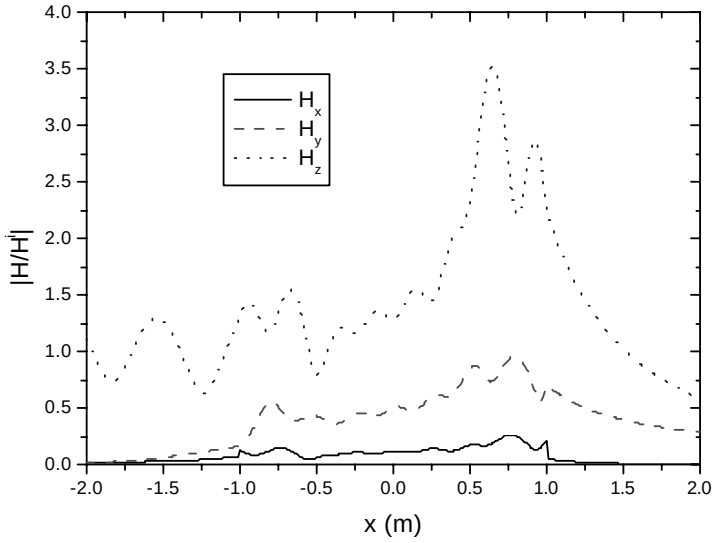

(c)

Figure 5. The co-polarized and cross-polarized bistatic RCS (a) and near-zone electric (b) and magnetic (c) fields of a GBM cylinder for a TE incident plane wave.

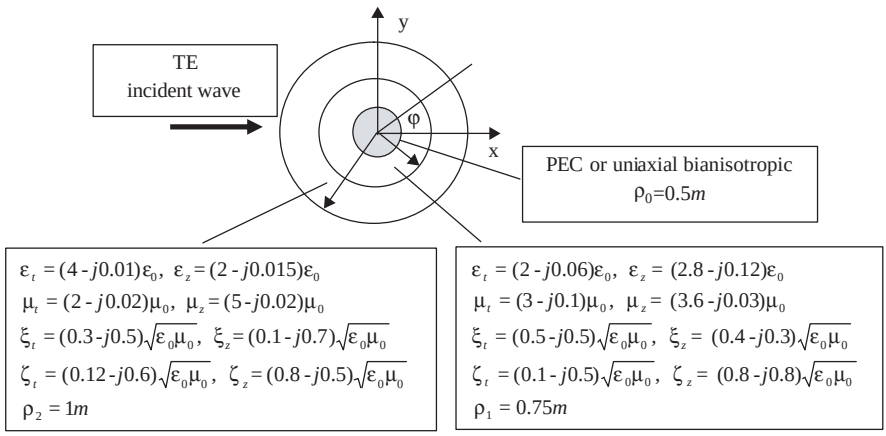

Figure 6. A two-layer uniaxial bianisotropic with/without PEC core cylinder.

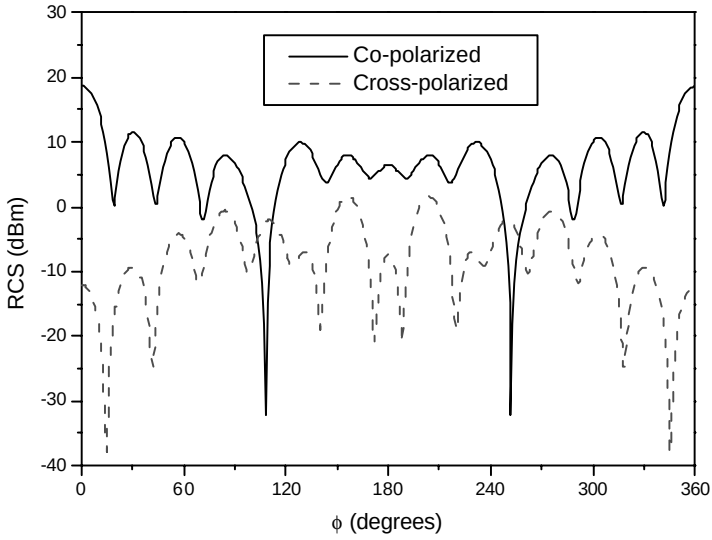

(a)

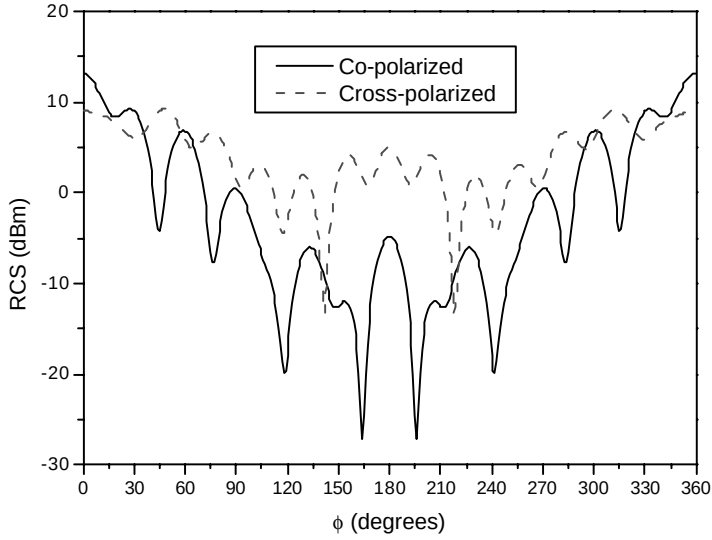

(b)

Figure 7. The co-polarized and cross-polarized bistatic RCS of a two-layer uniaxial bianisotropic cylinder (a) with and (b) without PEC center cylinder for a TE incident plane wave.

shows the bistatic RCS of this cylinder with the PEC center cylinder replaced by the same material as the inner layer uniaxial bianisotropic cylinder.

4. CONCLUSION

In this paper, we present a general formulation for the solution of electromagnetic scattering by a multilayer gyrotropic biansotropic circular cylinder for TM and TE incident plane waves using the eigenfunction expansion method. The numerical results including bistatic co-polarized and cross-polarized RCS and near-zone fields for three examples are presented. The results for the chiral cylinder agrees exactly with published results as our formulation collapses to that of [5] for chiral medium. The radar cross sections and near-field electric and magnetic fields of a gyrotropic bianisotropic circular cylinder and a two-layer uniaxial bianisotropic cylinder are also presented.

REFERENCES

1. Bohren, C. F., "Light scattering by an optically active sphere," *Chem. Phys. Lett.*, Vol. 29, 458–462, 1974.
2. Bohren, C. F., "Scattering of electromagnetic waves by an optically active cylinder," *J. Colloid Interface Sci.,* Vol. 66, 105–109, 1978.
3. Uslenghi, P. L. E., "Scattering by an impedance sphere coated with chiral layer," *Electromagn.,* Vol. 10, 201–211, Jan.–June 1990.
4. Kluskens, M. S. and E. H. Newman, "Scattering by a chiral cylinder of arbitrary cross section," *IEEE Trans. Antennas Propagat.,* Vol. 38, 1448–1455, Sept. 1990.
5. Kluskens, M. S. and E. H. Newman, "Scattering by a multilayer chiral cylinder," *IEEE Trans. Antennas Propagat.,* Vol. 39, 91–96, Jan. 1991.
6. Zhang, M. and W. X. Zhang, "Scattering of electromagnetic waves from a chiral cylinder of arbitrary cross section — GMT approach," *Microwave & Opt. Technol. Lett.,* Vol. 10, No. 1, 25, 1995.
7. Al-Kanhal, M. A. and E. Arvas, "Electromagnetic scattering from a chiral cylinder of Arbitrary cross section," *IEEE Trans. Antennas Propagat.,* Vol. 44, 1041–1048, July 1996.
8. Monzon, J. C., "Scattering by a biisotropic body," *IEEE Trans. Antennas Propagat.,* Vol. 43, 1288–1296, Nov. 1995.

9. Zhang, M. and W. Hong, "Electromagnetic scattering by a bianisotropic cylinder," *Proc. IEEE Antennas Propagat. Soc. Int. Symp.,* 910–913, Montreal Canada, July 1997.
10. Cheng, D. J., "Vector-wave-function theory of uniaxial bianisotropic semiconductor material," *Phys. Rev. E,* Vol. 56, No. 2, 2321–2324, 1997.
11. Yin, W. Y. and L. W. Li, "Multiple scattering from gyrotropic bianisotropic cylinders of arbitrary cross sections using the modeling technique," *Phys. Rev. E,* Vol. 60, No. 1, 918–925, 1999.
12. Shanker, B., S. K. Han, and E. Michielssen, "A fast multipole approach to analyze scattering from an inhomogeneous bianisotropic object embedded in a chiral host," *Radio Sci.,* Vol. 33, No. 1, 17–31, 1998.
13. Olyslager, F., "Time-harmonic two- and three-dimensional closed-form Green's dyadics for gyrotropic, bianisotropic and anisotropic media," *Electromagn.,* Vol. 17, No. 4, 369–386, 1997.
14. Olyslager, F., "Time-harmonic two- and three-dimensional Green dyadics for a special class of gyrotropic bianisotropic media," *IEE Proc. Microw. Antennas Propag.,* Vol. 143, No. 5, 413–416, Oct. 1996
15. Beker, B., K. R. Umashankar, and A. Taflove, "Numerical analysis and validation of the combined field surface integral equations for electromagnetic scattering by arbitrary shaped two-dimensional anisotropic objects," *IEEE Trans. Antennas Propagat.,* Vol. 37, No. 12, 1573–1581, Dec. 1989.